



**HAL**  
open science

## The Low-Threshold Calcium Channel Cav3.2 Determines Low-Threshold Mechanoreceptor Function

Amaury François, Niklas Schüetter, Sophie Laffray, Juan Sanguesa, Anne Pizzoccaro, Stefan Dübel, Annabelle Mantilleri, Joël Nargeot, Jacques Noël, John N. Wood, et al.

► **To cite this version:**

Amaury François, Niklas Schüetter, Sophie Laffray, Juan Sanguesa, Anne Pizzoccaro, et al.. The Low-Threshold Calcium Channel Cav3.2 Determines Low-Threshold Mechanoreceptor Function. Cell Reports, 2015, 10 (3), pp.370-382. 10.1016/j.celrep.2014.12.042 . hal-01109938

**HAL Id: hal-01109938**

**<https://hal.science/hal-01109938>**

Submitted on 12 Apr 2018

**HAL** is a multi-disciplinary open access archive for the deposit and dissemination of scientific research documents, whether they are published or not. The documents may come from teaching and research institutions in France or abroad, or from public or private research centers.

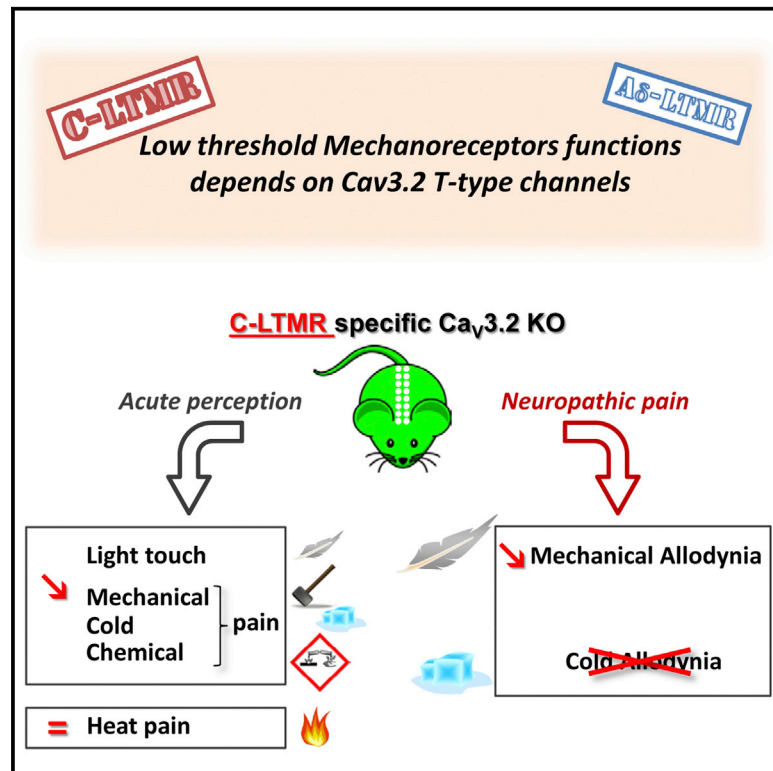
L'archive ouverte pluridisciplinaire **HAL**, est destinée au dépôt et à la diffusion de documents scientifiques de niveau recherche, publiés ou non, émanant des établissements d'enseignement et de recherche français ou étrangers, des laboratoires publics ou privés.



Distributed under a Creative Commons Attribution 4.0 International License

## The Low-Threshold Calcium Channel Cav3.2 Determines Low-Threshold Mechanoreceptor Function

### Graphical Abstract



### Authors

Amaury François, Niklas Schüetter, ..., Olaf Pongs, Emmanuel Bourinet

### Correspondence

emmanuel.bourinet@igf.cnrs.fr

### In Brief

François et al. show that Cav3.2 calcium channels are potent and specific regulators of low-threshold mechanoreceptors (LTMRs) setting the efficient detection, conduction, and transfer of tactile/pain information. In C-LTMRs, this mechanism crucially contributes to neuropathic pain, highlighting the utility of a therapeutic Cav3.2-inhibition strategy to improve patient quality of life.

### Highlights

- Cav3.2 calcium channels are markers of both C- and Aδ- low-threshold mechanoreceptors
- Cav3.2 in receptive fields and axons facilitates action potential initiation and conduction
- Cav3.2 in C-LTMR governs innocuous touch, noxious mechanical cold, and chemical pain
- Cav3.2 channels in C-LTMRs are molecular substrates of allodynia in neuropathic pain



# The Low-Threshold Calcium Channel Cav3.2 Determines Low-Threshold Mechanoreceptor Function

Amaury François,<sup>1,2,3,4</sup> Niklas Schüetter,<sup>5</sup> Sophie Laffray,<sup>1,2,3,4</sup> Juan Sanguesa,<sup>1,2,3,4</sup> Anne Pizzoccaro,<sup>1,2,3,4</sup> Stefan Dubel,<sup>1,2,3,4</sup> Annabelle Mantilleri,<sup>6</sup> Joel Nargeot,<sup>1,2,3,4</sup> Jacques Noël,<sup>1,7</sup> John N. Wood,<sup>8</sup> Aziz Moqrich,<sup>6</sup> Olaf Pongs,<sup>5</sup> and Emmanuel Bourinet<sup>1,2,3,4,\*</sup>

<sup>1</sup>Laboratories of Excellence, Ion Channel Science and Therapeutics, Institut de Génomique Fonctionnelle, 141 rue de la Cardonille, 34094 Montpellier, France

<sup>2</sup>CNRS UMR5203, 34095 Montpellier, France

<sup>3</sup>INSERM, U661, 34095 Montpellier, France

<sup>4</sup>Université de Montpellier, 34095 Montpellier, France

<sup>5</sup>Department of Physiology, University of Saarland, School of Medicine, Kirrberger Straße 1, 66424 Homburg, Germany

<sup>6</sup>Aix-Marseille-Université, CNRS, Institut de Biologie du Développement de Marseille, UMR 7288, 13288 Marseille, France

<sup>7</sup>Université de Nice Sophia Antipolis, Institut de Pharmacologie Moléculaire et Cellulaire, UMR7275 CNRS, 660 route des Lucioles, 06560 Valbonne, France

<sup>8</sup>Wolfson Institute for Biomedical Research, University College London, Gower Street, London WC1E 6BT, UK

\*Correspondence: [emmanuel.bourinet@igf.cnrs.fr](mailto:emmanuel.bourinet@igf.cnrs.fr)

<http://dx.doi.org/10.1016/j.celrep.2014.12.042>

This is an open access article under the CC BY-NC-ND license (<http://creativecommons.org/licenses/by-nc-nd/3.0/>).

## SUMMARY

The T-type calcium channel Cav3.2 emerges as a key regulator of sensory functions, but its expression pattern within primary afferent neurons and its contribution to modality-specific signaling remain obscure. Here, we elucidate this issue using a unique knockin/flox mouse strain wherein Cav3.2 is replaced by a functional Cav3.2-surface-ecliptic GFP fusion. We demonstrate that Cav3.2 is a selective marker of two major low-threshold mechanoreceptors (LTMRs), A $\delta$ - and C-LTMRs, innervating the most abundant skin hair follicles. The presence of Cav3.2 along LTMR-fiber trajectories is consistent with critical roles at multiple sites, setting their strong excitability. Strikingly, the C-LTMR-specific knockout uncovers that Cav3.2 regulates light-touch perception and noxious mechanical cold and chemical sensations and is essential to build up that debilitates allodynic symptoms of neuropathic pain, a mechanism thought to be entirely A-LTMR specific. Collectively, our findings support a fundamental role for Cav3.2 in touch/pain pathophysiology, validating their critical pharmacological relevance to relieve mechanical and cold allodynia.

## INTRODUCTION

Somatosensory perception is dependent on a variety of primary sensory neurons that are able to detect and transmit sensations, which range from hedonic to painful (Basbaum et al., 2009; Lallmend and Ernfor, 2012; Liu and Ma, 2011). Deciphering this complex neuronal diversity is a key challenge in sensory neuro-

biology. One intriguing facet is the role of the cutaneous mechanosensors that discriminate innocuous and noxious mechanical forces and respectively translate them into touch or pain sensations. Moreover, in the development of pathological pain, normal tactile signaling of low-threshold mechanoreceptors (LTMRs) is converted into sensations of pain. As LTMRs encompass different neuron subclasses, decoding the mechanisms that determine their sensitivity and their contribution to pain pathologies is critical to the development of future analgesic treatments.

Fast-conducting myelinated axons and large cell bodies characterize A-fiber-associated sensory neurons (A $\alpha$ ,  $\beta$ , or  $\delta$ ), which are involved mostly in touch and proprioception. Slowly conducting unmyelinated fibers with small cell bodies correspond to C-fibers involved in not only nociception but also conveying tactile information. LTMRs are heterogeneous; comprise A $\beta$ -, A $\delta$ -, and C-fiber subtypes; and are further subdivided according to their rate of adaptation to mechanical stimuli and by their distal and central terminal anatomy (Li et al., 2011). However, molecular markers of LTMRs remain insufficient to fully decipher their pathophysiological roles. Recently, a small population of unmyelinated dorsal root ganglia (DRG) neurons has been described for their unique expression of tyrosine hydroxylase (TH), vesicular transporter of glutamate 3 (VGLUT3), and chemokine like protein TFAA4 (Brumovsky et al., 2006; Delfini et al., 2013; Seal et al., 2009). These neurons represent the poorly understood population of C-LTMRs involved in apparently opposing sensations of pleasant touch and hypersensitivity during chronic pain (Bessou et al., 1971; Seal et al., 2009). Another specific population of LTMRs is the TrkB-expressing neurons innervating D-hair follicles and described as A $\delta$ -LTMRs. Interestingly, these neurons express the Cav3.2 isoform of low-voltage-activated calcium channels (Shin et al., 2003).

This channel belongs to a gene family composed of three members (Cav3.1, 3.2, and 3.3), with Cav3.2 being predominant in DRGs. They activate at low voltages close to the membrane

resting potentials and therefore are important tuners of cell excitability (Perez-Reyes, 2003). A constitutive Cav3.2 knockout (KO) in mice impairs A $\delta$ -LTMRs excitability (Wang and Lewin, 2011). In addition, electrophysiological analyses shows that Cav3.2 has a proexcitatory impact in small-diameter nociceptors expressing mechanoactivated channels (Coste et al., 2007). In Cav3.2 KO mice, intrathecal antisense-mediated Cav3.2 knockdown and the use of T-type channel antagonists induce a marked analgesia in vivo (Bourinet et al., 2005; Choe et al., 2011; Choi et al., 2007; François et al., 2014). Conversely, enhanced Cav3.2 activity parallels chronic pain states (García-Caballero et al., 2014; Jagodic et al., 2008; Marger et al., 2011; Messinger et al., 2009; Takahashi et al., 2010).

However, to unravel the complete role of Cav3.2 within all the sensory neuron classes, several fundamental anatomical and functional questions still remain to be addressed. The aim of the present work is to determine the contribution of Cav3.2 to pathophysiological somatosensory signaling within DRG neuron subtypes by elucidating how its subcellular location affects information processing in sensory fibers.

To investigate this, we designed a knockin (KI) strategy by inserting a two *loxP* site-flanked eYFP tag into exon 6 of the Cav3.2 locus to allow genetic marking of Cav3.2 channels as well as tissue-specific loss of function. Interestingly, our analysis shows that Cav3.2 is a selective marker for mechanoreceptors comprising the C- and the A $\delta$ -LTMRs expressing TH/VGLUT3/TAFA4 and TrkB, respectively, in addition to a third population of Ret-positive neurons that do not coexpress any of the classical markers for peptidergic and nonpeptidergic C-fibers. We also show that Cav3.2 is localized within the putative zone of action potential (AP) generation, in the vicinity of hair follicles in distal nerve endings. Furthermore, it is also expressed along the axons of afferent C-LTMR fibers and in the nodes of Ranvier of A $\delta$ -LTMRs and also both pre- and postsynaptically in the dorsal horn lamina II–III of the spinal cord. Functional analysis of C-LTMR in cutaneous fibers shows that T-type channels determine their low threshold of mechanical activation and accelerate AP conduction along the axon.

Finally, the pathophysiological role of Cav3.2 within C-LTMRs was assessed by generating a conditional Cav3.2 KO using Nav1.8-Cre mice to eliminate Cav3.2 selectively from C-fibers. We show here that Cav3.2 determines the basal high sensitivity of C-LTMRs, regulating innocuous and noxious mechanical and cold detection as well as chemically induced pain. Moreover, our data demonstrate that C-LTMRs expressing Cav3.2 contribute to both mechanical and cold allodynia in peripheral neuropathy. In contrast to the canonical view that only myelinated tactile afferences encode allodynia, our work refines this view by providing molecular clues for the contribution of C-tactile fibers and validates Cav3.2 as a pertinent target to dampen debilitating aspects of pathological pain.

## RESULTS

### A Mouse Model to Investigate Cav3.2 Function in Sensory Neurons

To understand Cav3.2 function within sensory neuron subtypes, we engineered a knockin mouse with a fusion of a pH-sensitive

GFP (eYFP-GFP; Miesenböck et al., 1998) within the large extracellular loop preceding the P loop in the first transmembrane domain of the channel (Figures 1A–1C). Homozygous mice harboring this insertion (hereafter named KI) are viable and fertile, born in a Mendelian ratio, and indistinguishable from their control littermates. Importantly, the recombinant allele allowed correct transcription and translation of the fusion protein (Figures 1D, 1E, and S1A–S1C) as well as fine localization of expressed channels (Figures S1D, S1E, and S2). Electrophysiological analysis of native currents in A $\delta$ -LTMRs cells, recognizable by their rosette morphology in culture, showed no differences in T-type calcium current amplitudes and kinetics between wild-type (WT) and homozygous KI/KI mice (Figures 1F and 1G) or in voltage-dependent properties (Figures S1F and S1G). Altogether, these results suggest no abnormalities in function and membrane expression of Cav3.2-GFP channels in KI mice.

### Cav3.2-Expressing Neurons Display Properties of A $\delta$ - and C-LTMRs

As the Cav3.2-GFP protein faithfully recapitulates Cav3.2 transcript expression, we deciphered the cellular distribution of Cav3.2 protein in DRG neurons and correlated this pattern with specific sensory modalities. Double immunostaining of GFP with PGP9.5 (a general neuronal marker) identified GFP immunoreactivity (GFP-IR) in 33% of all L4 DRGs (Figure 2A). Cav3.2-GFP+ neurons segregate into two classes: neurofilament NF200+ representing 28% and peripherin+ representing 66% of all Cav3.2-expressing neurons (Figure S2A). The subset of large NF200+/Cav3.2-GFP+ neurons exclusively express TrkB, the main marker of A $\delta$ -LTMR (Figure 2B), while those expressing peripherin (an unmyelinated fiber marker) could be further subdivided into neurons containing C-LTMR markers such as TAFA4, VGLUT3, and TH and an as yet to be identified population of Ret+ neurons that express none of the markers tested so far (Figures 2 and S2). Coexpression with TrkA, CGRP, and TRPV1 remained minor in all cases (Figure 2G). Hence, Cav3.2 is expressed in major populations of mechanoreceptors.

We next used live GFP labeling of Cav3.2-expressing neurons to decipher their physiological properties in culture. Mechanical stimulation of the Cav3.2-GFP+ neuron cell soma evoked inward mechanoactivated (MA) currents in all neurons tested. As previously described, MA currents have different adaptation rates (Figure 3A) (Delmas et al., 2011). Interestingly, rapidly and intermediately adapting currents (RA and IA, respectively) were predominantly found in large GFP+ neurons, whereas slowly adapting (SA) and ultraslowly adapting (USA) currents predominate in smaller GFP+ neurons (Figure 3B). Among the candidate substrates for MA channels, piezo2, which shows RA kinetics in recombinant systems, is highly expressed in Tafa4/Cav3.2-positive neurons (Figure S3), suggesting their possible contribution to the SA/USA MA currents as well (but see Lou et al., 2013). Kinetics of MA currents uniquely shapes cell firing from phasic to tonic spiking, properties identified in the distinct LTMR fiber subtypes (Woodbury et al., 2001). Given that Cav3.2-GFP marks C-LTMRs and A $\delta$ -LTMRs, we tested the occurrence of these firing properties in GFP+ neurons. Consistent with the slow adaptation of MA currents, mechanical stimulation triggered tonic AP firing in small GFP+ neurons. Furthermore, cooling also elicited firing in

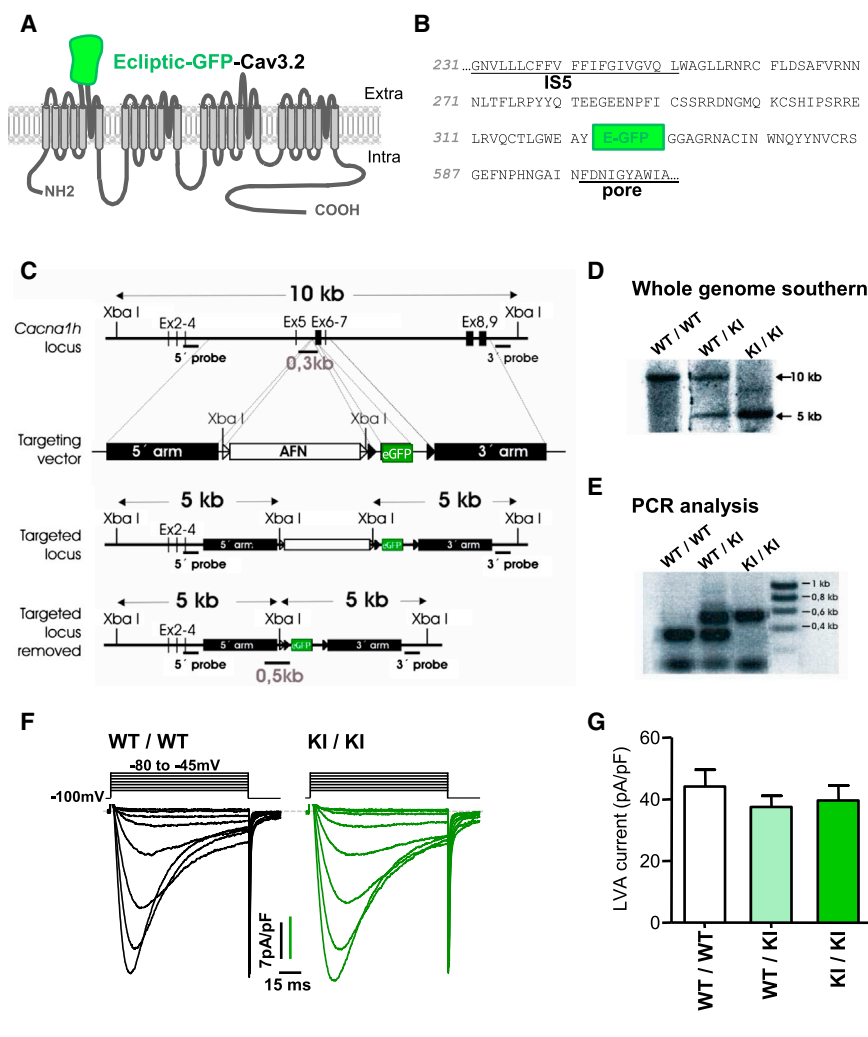


**Figure 1. Generation and Analysis of Cav3.2-GFP Knockin Mice**

(A) Scheme of the Cav3.2-ecliptic-GFP fusion structure.

(B) Segment of the murine Cav3.2 protein sequence. The ecliptic-GFP is inserted in the extracellular loop between the fifth transmembrane segment (IS5) and the pore region.

(C) Schematic diagram to illustrate the *cacna1h* targeting strategy. *Cacna1h* locus: black vertical bars depict the exons (Ex) structure from 2 to 9 of the murine *cacna1h* gene. Targeting vector: the 5' and 3' arms each consist of ~2.5 kb of genomic sequence. Open triangles mark FRT sites surrounding neomycin resistance cassette (AFN). eGFP displays ecliptic-GFP insertion. Filled triangles mark *loxP* sites inserted before exon 6 and after exon 7. Black bars beneath the genomic sequences illustrate Southern probes and PCR fragments used for genotyping. Targeted locus: scheme displays insertion of targeting vector into the *cacna1h* locus. Targeted locus AFN removed: sequence between FRT sites after AFN excision with Flipase. Lines with arrowheads depict XbaI restriction fragments.

(D) Southern analysis of wild-type (WT/WT), heterozygous (WT/KI), and homozygous mutant (KI/KI) mouse DNA. Genomic DNA was digested with XbaI. The 3' probe was used for the detection of restriction fragments. Arrows mark positions of wild-type (10 kb) and mutant (5 kb) bands.

(E) Genotyping results of a PCR assay performed on genomic DNA. A 0.5 kb band demonstrates excision of AFN cassette.

(F) Analysis of Cav3.2-mediated low-voltage-activated calcium currents in medium-sized DRG neurons of KI/KI and WT/WT genotypes.

(G) Mean current densities in WT/WT-, WT/KI-, and KI/KI-derived cells identified by their rosette morphology.

Data are presented as mean  $\pm$  SEM.

these neurons ( $n = 9$ ), a hallmark of C-LTMR fibers (Li et al., 2011; Takahashi et al., 2003) (Figure 3C). In contrast, none of the neurons tested responded to warming (not shown). Comparatively, large GFP+ neurons systematically responded to mechanical stimuli with a single spike phasic to the stimulus onset (Figure 3D). Neither cooling nor warming excited these neurons ( $n = 10$ ). In parallel, we were unable to detect any intracellular calcium level variations when we challenged neurons with thermo TRP channels or Mrgp receptor agonists, with the exception of the TRPA1 agonist AITC that induced small responses in some small GFP+ neurons (not shown).

To confirm the distinct cellular firing of Cav3.2-GFP-expressing LTMRs, we used mechanical stimuli of various velocities. Small Cav3.2-GFP+ neurons responded better to slow-motion stimuli consistent with the physiological properties of C-LTMRs (Figure 3E), as previously described for TFAFA4+ neurons (Delfini et al., 2013) and further demonstrated in Cav3.2-GFP+/TFAFA4-GFP+ neurons from double-heterozygote mice (Figure 3F). In contrast, large GFP+ neurons only responded to fast mechanical stimuli, as A $\delta$ -LTMR do (Abraira and Ginty, 2013). Figure 3F summarizes these observations by presenting the probe velocity

eliciting the first spike, as a function of cell capacitance. Two populations can be distinguished from each other: the large neurons stimulated by fast stimuli, and the small neurons stimulated preferentially by slow mechanical stimuli. Of note in this latter group, the TFAFA4-GFP+ and the TFAFA4-GFP- neurons are similarly activated, and they all behave as C-LTMRs.

### Cav3.2 Is Expressed in Fiber Compartments Critical for AP Initiation and Propagation

Primary sensory neurons consist essentially of peripheral and central terminal arbors as well as long axons within nerve bundles. Therefore, deciphering the Cav3.2-GFP subcellular localization is essential to understanding channel function(s). Analyses of GFP-IR in distal nerve terminals revealed the channel presence in fibers innervating hairy skin. Using S100 as a marker of terminal Schwann cells surrounding nerve endings, we could detect GFP-IR in close proximity to lanceolate structures around hair follicles (Figure 4A). Magnification shows an intense GFP-IR nearby the branching points where daughter nerve endings join each other. Interestingly, Cav3.2-GFP detection along teased fibers of sciatic nerve, revealed strong GFP-IR in the nodes of

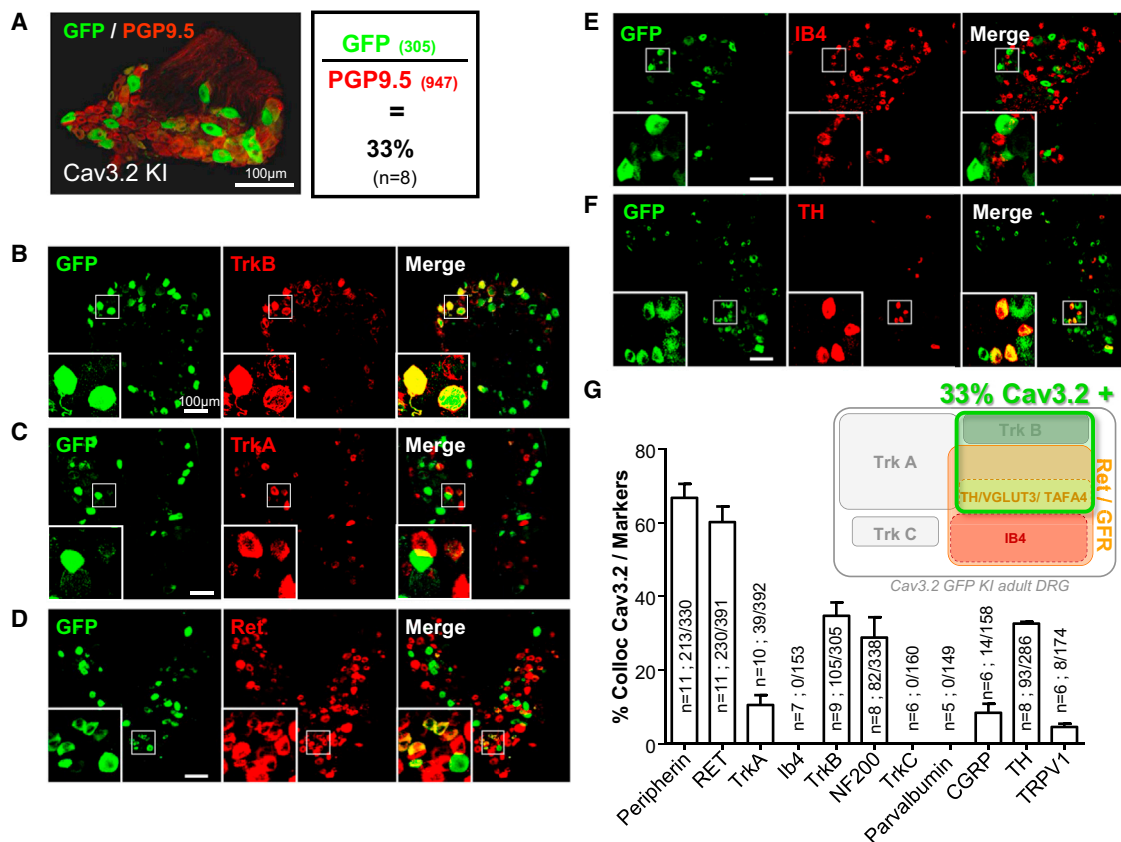


### Figure 2. Sensory Neuron Classes Expressing Cav3.2

Adult L4 DRG sections from Cav3.2-GFP KI mice costained with anti-GFP antibodies (green) and anti-PGP9.5 (red) (A), anti-TrkB (B), anti-TrkA (C), anti-Ret (D), isolectin B4 (E), and anti-tyrosine hydroxylase (TH) (F). In all panels, insets are magnified views of indicated areas within white boxes. Scale bar, 100 µm. Quantitative data of colocalization between markers are shown in (G). In each histogram bar, “n” indicates the number of animals used, followed by the total number of neurons colabeled with the specific marker over the total number of Cav3.2-GFP cells. Data are presented as mean ± SEM. The cartoon is a representative view of the Cav3.2 population in adult DRG, in accordance with the different markers described.

Ranvier of some medium caliber axons flanked with paranodin labeling and overlapping with KCNQ2 staining (paranode and node markers, respectively) (Figure 4B). Concerning thin unmyelinated C-fibers, the GFP-IR signal was observed all along axons (Figure 4B, empty arrows) overlapping with peripherin (Figure S4A). We found a similar localization pattern in dorsal roots purely composed of sensory afferences (Figure 4C). In contrast, efferent axons in ventral roots did not show any GFP-IR (Figure S4B). In the ganglia, GFP-IR was detected in the proximal unmyelinated segment linking the cell soma to the axon in all Cav3.2-GFP+ neurons (Figure 4D). Thus, the channel is present from the periphery, throughout the length of the axons with a specific enrichment at locations key to cell excitability.

GFP-IR was examined in the dorsal horn of the spinal cord and a strong signal was observed in the laminae II–III with an overlap with PKCγ-containing interneurons (Figure 4E). Although the GFP-IR may result from both afferent endings and spinal neurons, the labeling is consistent with Aδ- and C-LTMR input zones with little overlap with IB4+ or CGRP+ C-nociceptive inputs in the outer lamina II or lamina I or with parvalbumin+ Aβ inputs in laminae III–IV (Figures S4C and S4D). More precise localization using

transmission electron microscopy (TEM) revealed GFP-IR in the lamina II–III synapses. Examination of more than 50 different identified synapses shows that the most intense labeling was detected on the postsynaptic area compared to the presynaptic zone (Figure 4F).

### Cav3.2 Controls Mechanosensitivity Threshold and AP Propagation in C-LTMRs

Since we aimed to investigate Cav3.2 function in C-fibers in vivo using a conditional loss-of-function approach, we next examined the role of peripheral Cav3.2 channels in C-LTMRs using the skin-nerve recording technique. Application of light mechanical stimuli on C-fibers successfully identified C-LTMRs with firing thresholds below 10 mN (Figures 5A and 5B), slowly adapting firing, and pronounced after discharges as previously reported (Vallbo et al., 1999). Next, we used TTA-A2, a selective T-type calcium channel antagonist (Francois et al., 2013). Local blockade of Cav3.2 in fiber receptive fields induced a significant elevation of the C-LTMR activation threshold and a reduction of AP firing frequency (Figures 5A, 5B, and S5), therefore shifting the firing characteristics toward those of high threshold

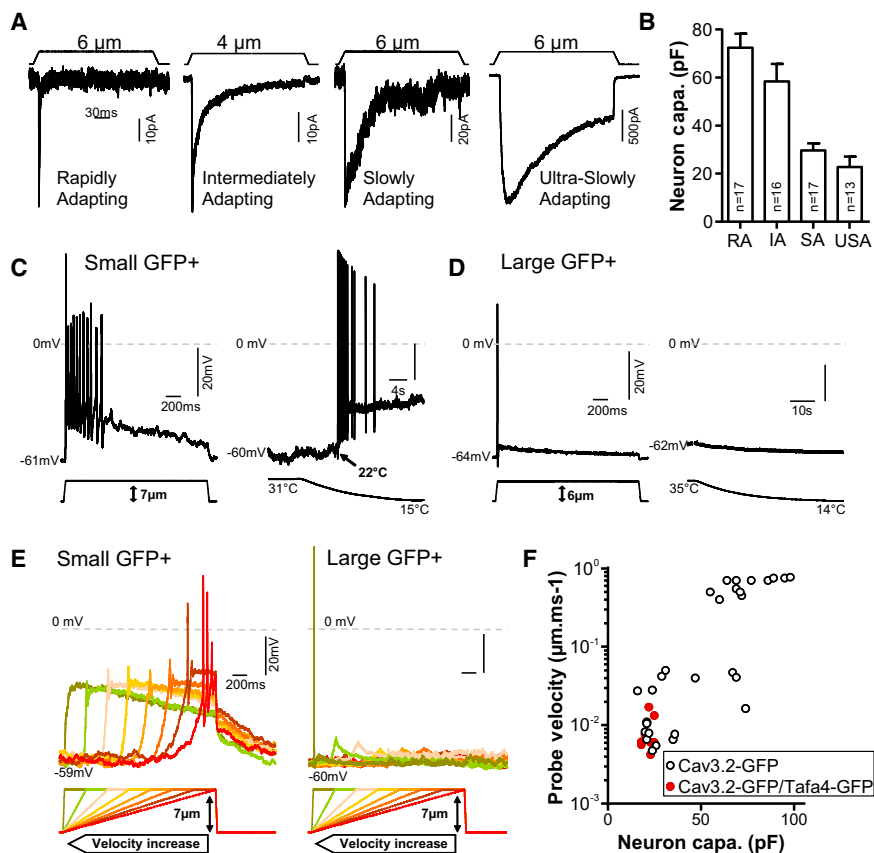


**Figure 3. Mechanical Modalities in Cav3.2-Expressing Neurons**

(A) Representative traces of mechanically-activated (MA) currents in GFP+ DRG neuron soma in culture, elicited by a piezoelectric-driven probe stimulation. The traveled distance by the probe is indicated on the top of each trace (in  $\mu\text{m}$ ). Time constants of current decay discriminate four types of MA currents classified as rapidly adapting (RA), intermediately adapting (IA), slowly adapting (SA), and ultraslowly adapting (USA).

(B) Cell size classification of recorded GFP+ neurons, according to their related capacitance (in pF,  $\sim 40$  pF being the limit between small and large neurons) as function of the MA current type they express. Data are presented as mean  $\pm$  SEM.

(C and D) Action potentials (AP) generated by mechanical stimulation (left) and cooling (right) in small (C) and large (D) GFP+ neurons. Mechanical and thermal stimulations are indicated below each trace.

(E) AP generation in small (left) and large (right) Cav3.2-GFP+ neurons with constant subthreshold mechanical stimulation applied at various velocities. Each color represents a different probe velocity applied sequentially from slow to fast.

(F) Probe velocity threshold eliciting an AP according to the cell size of the recorded Cav3.2-GFP+ neuron from Cav3.2-GFP KI (open black circles) and Cav3.2-GFP KI  $\times$  Tafa4-GFP double-heterozygote mice (red filled circles).

mechanoreceptor C-fibers (C-HTMR). In contrast, application of TTA-A2 had no effect on genuine C-HTMR (not shown). The presence of Cav3.2 along C-LTMR axons suggests a potential role in AP conduction velocity (CV). Indeed, application of TTA-A2 on the entire skin-nerve preparation to target axonal Cav3.2, slowed significantly the CV with minimal effect on the AP shape, supporting the presence of functional axonal Cav3.2 channels (Figures 5C and 5D).

### Generation of a Conditional Cav3.2 Knockout Mouse

*loxP* sites within the KI were designed to trigger tissue-specific Cav3.2 gene inactivation. Partnering the KI animals with mice expressing Cre recombinase under the Nav1.8 promoter (Stirling et al., 2005) allowed deletion of Cav3.2 specifically in small-diameter DRG neurons (mice hereafter named SNS KO). As for the KI, SNS KO are born in a Mendelian ratio, survive to adulthood, and are indistinguishable from their KI littermates. Figure 6A shows a perfect overlap between Nav1.8 and small-diameter Cav3.2-GFP+ neurons in KI DRGs while this double labeling is completely lost in SNS KO. Consistently, the number of Cav3.2-GFP+ neurons dropped from 33% to  $13.9\% \pm 1.7\%$  (Figure 6B). GFP costaining with specific markers indicated that recombination mainly occurred in small-diameter Ret+ neurons (Figure 6E) and, most importantly, in all TH+ C-LTMRs (Figure 6F). This indicates effective Cav3.2 loss of function in this population, without affecting TrkB+ neurons (Figures 6C, 6D, 6G, 6H, and

S6A–S6E). Accordingly, T-type currents are unaffected in SNS KO A $\delta$ -LTMRs (Figures S6A and S6B), and live staining of surface-expressed Cav3.2-GFP revealed a selective channel disappearance in small neurons sparing the A $\delta$ -LTMRs (Figures S6C–S6E). Taken together, our data demonstrate that the SNS KO mouse model represents a powerful tool to decipher the role of peripheral Cav3.2 in the pathophysiology of C-LTMRs.

### Cav3.2 in C-LTMR Controls Innocuous and Noxious Mechanical/Cold Perception and Pathological Pain

To investigate whether SNS KO had modified mechanical perception, we subjected these mice to a wide range of innocuous and noxious mechanical stimuli. We first used three static von Frey filaments corresponding to innocuous, intermediate, and noxious stimulations (0.07 g, 0.6 g, and 1.4 g respectively) and generated a normalized withdrawal score. SNS KO mice had a reduced score for the intermediate filament, indicative of a dampened light-touch sensitivity (Figure 7A). Similarly, determination of the von Frey paw withdrawal threshold (PWT; up and down method) showed a tactile deficit in SNS KO (Figure 7H, PWT before spared nerve injury model [SNI] surgery). Differences between SNS KO mice and their KI littermates are not due to motor or coordination deficits (Figure S7D). The animal's ability to respond to painful mechanical stimuli of stronger intensities was tested with two additional paradigms: the dynamic von Frey (esthesiometer) and the Randall-Selitto test. In both

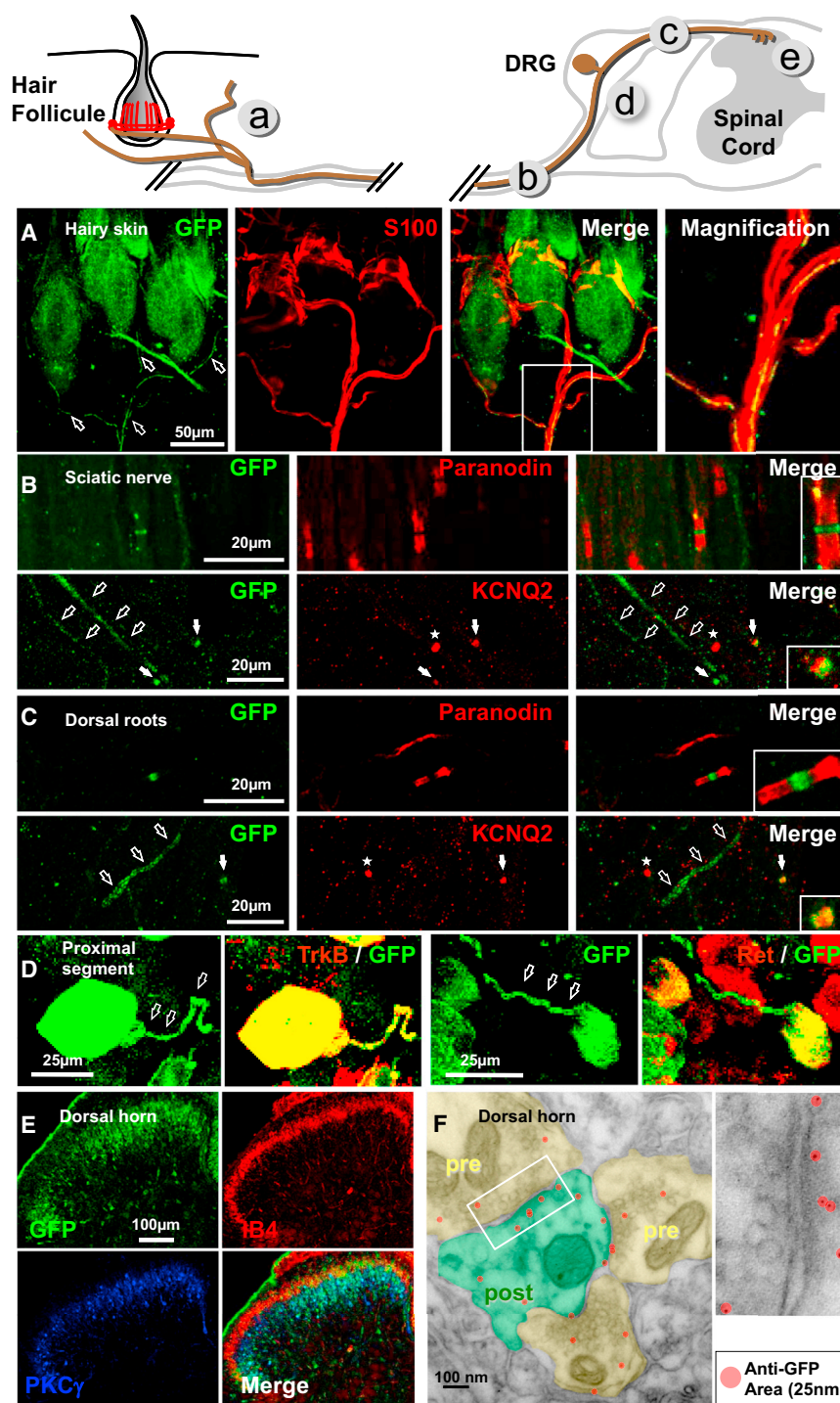


**Figure 4. Subcellular Localization of Cav3.2 in Primary Sensory Neurons**

Representation of the different sensory neuron subcellular localizations explored for Cav3.2-GFP expression in adult KI mice.

(A) Hairy skin whole-mount immunostaining of Cav3.2-GFP (green) and Schwann cell marker S100 (red) in KI mice. Empty arrows indicate nerves innervating hair follicles forming lanceolate endings. The right panel is a magnification of the box on the merge image.

(B and C) Teased fibers costained with Cav3.2-GFP (green), paranodin (red, top), or KCNQ2 (red, bottom) in the sciatic nerve (B) or dorsal roots (C). Nodes of Ranvier that express Cav3.2 in their center are indicated by filled arrows, while Cav3.2 negative nodes of Ranvier are indicated by asterisks. Empty arrows represent Cav3.2-GFP immunoreactivity in small unmyelinated fibers.

(D) Cav3.2-GFP+ DRG soma positive for TrkB (left) or Ret (right) at high magnification. Empty arrows indicate the presence of Cav3.2-GFP in the axon proximal segment.

(E) Lumbar spinal cord dorsal horn section from Cav3.2-GFP KI mice costained for GFP (green), IB4 (in red, marking lamina II inner), and PKC $\gamma$  (blue, marking lamina II/inner-III).

(F) Transmission electron microscopy (TEM) images from pre-embedded GFP silver staining of spinal cord dorsal horn coronal sections. Red dots represent GFP antibody complexes around individual silver dot (25  $\mu$ m). Areas in yellow are presynaptic regions containing dense synaptic vesicles. Green area is a postsynaptic region recognized by the postsynaptic density. Right panel is a magnification of the box in the left image.

the dynamic cold- and hot-plate tests, and a thermotaxis assay. In agreement with the expression of Cav3.2-GFP in cold-sensitive small DRG soma (Figure 3C), SNS KO exhibited a decreased cold sensitivity in the paw immersion test (Figure 7D), a diminished escape behavior to noxious cold temperatures in the dynamic cold-plate test (Figure 7E), and a strong preference for cooler temperatures in the gradient test paradigm (Figures 7F and S7A), whereas acute innocuous cool stimulation with the acetone evaporation test ( $\sim 3^{\circ}\text{C}$ – $4^{\circ}\text{C}$  drop of skin temperature) did not reveal behavioral changes in control animals (Figure 7I, day 2 before SNI surgery).

tests, SNS KO displayed dampened responses to paw and tail pressure, respectively (Figures 7B and 7C). Altogether, our data demonstrate that Cav3.2 is required to respond to innocuous and noxious mechanical stimuli.

We next assessed the thermosensation phenotype in SNS KO mice. We subjected mice to a range of temperature sensation paradigms including paw immersion in hot and cold water baths,

To test whether Cav3.2 in C-LTMR fibers also plays a role in pathological pain, we first subjected mice to the formalin test. SNS KO exhibited significantly reduced first and second phase responses following formalin injection (Figure 7G), indicating the importance of Cav3.2-expressing C-LTMRs in this process related to both acute and inflammatory pain. Next, we assayed neuropathic pain with the SNI model (Decosterd and Woolf,

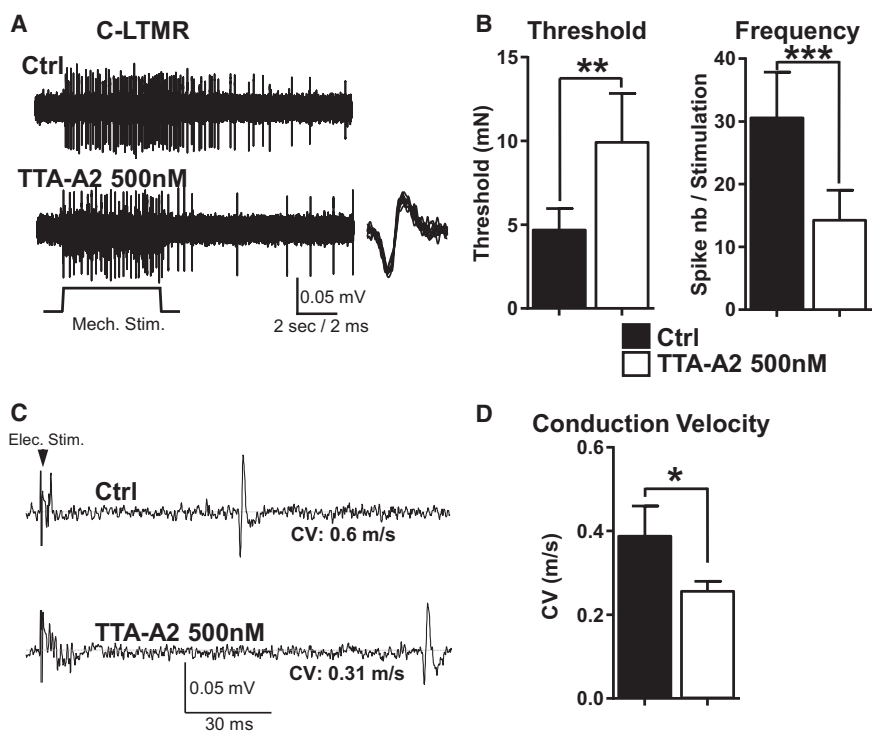


**Figure 5. Cav3.2 Tunes Mechanical Responses of Wild-Type Mouse C-LTMR**

(A) Representative nerve-skin recording of a C-LTMR fiber in response to a mechanical stimulation of its receptive field in the hairy skin. Response to a suprathreshold stimulation in control condition (top trace) or after local application of 500 nM TTA-A2 to the receptive field (bottom trace). Inset on the right is superposed magnifications of isolated AP from traces on the left in control and TTA-A2 situation.

(B) Summary of C-LTMR mechanical thresholds (left) and APs frequency (right) before and after application of 500 nM TTA-A2. Data are presented as mean ± SEM (\*\* $p < 0.01$  [ $n = 16$ ] for thresholds; \*\*\* $p < 0.001$  [ $n = 16$ ] for frequency; Wilcoxon signed rank test).

(C and D) Action of TTA-A2 on conduction velocity. The tonic action of TTA-A2 on the conduction velocity of a C-LTMR fiber (resting CV 0.6 m/s) is shown in (C), where 500 nM of TTA-A2 is applied to the entire recording chamber to have access to the nerve trunk and to the receptive field. Note that conduction velocity is decreased (CV 0.3 m/s in TTA-A2). (D) Histogram representation of conduction velocity before and after application of 500 nM TTA-A2. Data presented mean ± SEM. \* $p < 0.05$  ( $n = 4$ ); Wilcoxon signed rank test.

2000). We measured the increase in tactile and cold sensitivity in which innocuous stimuli illicit a pain response (allodynia), a phenomenon characteristic of neuropathic pain. Development of mechanical allodynia, demonstrated by the robust lowering of tactile thresholds in the KI mice (92% decrease) was significantly reduced in SNS KO by about a quarter (Figure 7H, day 14, and Figure S7B, 73% decrease only). However, since sensory perception is not linear but follows a logarithmic rule (Weber's law), the observed dampened allodynia in the lower end of the von Frey detection range has a great biological relevance (Mills et al., 2012). Correction for this law (as in Mills et al.'s statistics on the log PWT) accordingly increases the significance of SNS KO dampened mechanical allodynia (from  $p < 0.05$  (Figure 7H, D14) to  $p < 0.001$ ). Similarly, assessing sensitivity to innocuous skin cooling by the acetone evaporation test revealed a strong phenotype, since cold allodynia was abolished in SNS KO mice (Figure 7I). Although sex differences in neuropathic pain exist, both genders revealed the same phenotypes (Figures S7B and S7C), and thus male and female data were pooled (Figures 7H and 7I). Taken together, these results show that Cav3.2 channel activity in C-LTMR fibers is required for fine perception of multiple sensory modalities under both basal and pathological conditions.

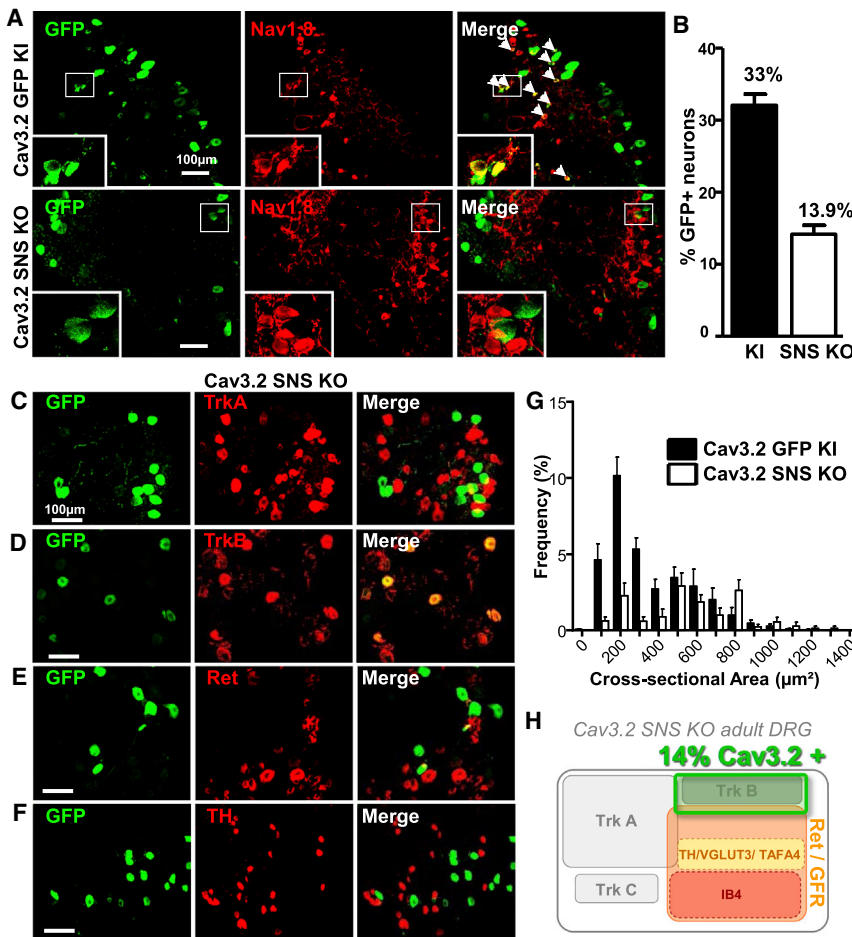
## DISCUSSION

Low-voltage-activated T-type calcium channels encoded by the Cav3.2 subunit have emerged as key elements of sensory neuron excitability in shaping both pain and tactile perception (Bourinet et al., 2014). However, deciphering how Cav3.2

achieves these functions requires assessment of their cellular and subcellular localization as well as the analysis of the impact of their functional loss in primary afferent neurons. To this end, we have used mouse genetics to knock in a surface GFP-tagged Cav3.2 channel together with an insertion of *loxP* sites into the *cacna1h* gene to generate tissue-specific conditional knockout animals. Our data demonstrate that this modification preserves the channel function, as the knockin mice express a fully functional ecliptic-GFP surface-tagged Cav3.2. Although several mouse models have been generated using cytosolic GFP-tagged membrane receptors or ligand gated channels, such an "all-in-one" extracellular ecliptic-GFP knockin-floxed mouse has not been reported for an ion channel before. Using this versatile model, we provide a comprehensive examination of the cellular distribution and functional relevance of the Cav3.2 channel in sensory processing, focusing on primary afferent neurons and the mechanistic rationale of its specific expression in defined subsets of LTMR neurons.

In the Cav3.2-GFP KI mouse, the tagged-channel expression is subjected to the same genetic regulation as the WT sequence since the 3' and the 5' regulatory regions are kept intact. Expression overlap between GFP signal and Cav3.2 mRNA, as well as similarity with previous in situ hybridization (Talley et al., 1999), unaffected current density, pharmacological properties, and normal animal behavior, indicated that the tagged channel is processed in the same manner as the wild-type Cav3.2.

GFP immunolabeling showed that Cav3.2-expressing neurons can be split into two distinct subsets of LTMRs: the  $A\delta$ - and the C-LTMRs, the first encompassing TrkB-positive and the latter



Ret-positive/IB4-negative neurons. These data are in sharp contrast with the recently described molecular characterization of Cav3.2-expressing neurons using a commercial anti-Cav3.2 antibody in DRG cultures (Rose et al., 2013). Limits of antibody specificity could explain this discrepancy, since the same anti-Cav3.2 antibody identified bands unrelated to Cav3.2 in our experiments (Figure S1B).

Functional analysis using electrophysiological recordings confirmed the expression pattern of Cav3.2-GFP neurons. They displayed MA currents with distinct adaptation rates. Medium-sized neurons had MA currents with rapid adaptation, typical of A $\delta$ -LTMRs, while the smaller neurons displayed SA MA currents, similar to that described for C-LTMRs. It is worth noting that the molecular characterization of these SA neurons can be split into TAF4<sup>+</sup>/TH<sup>+</sup> and a yet to be identified Ret<sup>+</sup>/IB4<sup>-</sup> population, suggesting a previously postulated heterogeneity within C-LTMRs (Delfini et al., 2013; Lou et al., 2013; Vrontou et al., 2013). Another feature of C-fibers expressing Cav3.2 is their enhanced excitability to cold/cool stimulation independently of the presence of TRPM8, as described for Nav1.8-containing neurons (Abrahamsen et al., 2008; Zimmermann et al., 2007). Altogether, we propose that C-LTMRs is a neuronal population of distinct identities, the majority of which express Cav3.2.

A $\delta$ - and C-LTMRs mainly innervate the hairy skin in the periphery with fork-shaped lanceolate endings interdigitated around the same two hair types, namely the zigzag and the awl/auchene hairs (98% of mouse fur hairs; Li et al., 2011). Moreover, the multiple sensory afferent terminal arbor morphologies revealed that C-tactile fibers are extremely branched, connect to a large number of distant hairs, and cover a large skin territory (Wu et al., 2012). This organization is well matched for an optimal stimulation by slowly moving stimuli. Generator potentials likely originate in axonal compartments, within or adjacent to lanceolate structures, when mechanosensors open following hair deflection. These potentials then spread from the daughter branches down into the parental nerve arbor where the AP firing threshold is reached (Hall and Treinin, 2011). While the site of AP initiation is not well defined in sensory endings, branching points are functionally important (Peng et al., 1999). In this context, we provide evidence for a preferential Cav3.2-GFP localization in distal nerve regions around fiber branching sites. Considering that T-type calcium channels activate before sodium channels, they are well positioned for lowering the excitability threshold and helping AP generation. This is indeed what isolated skin nerve experiments demonstrated as pharmacological T-type channel inhibition in C-LTMR receptive fields elevates their mechanical threshold. Similarly TTA-A2 increases the threshold of electrically evoked AP firing in Cav3.2 expressing DRG in culture (Francois et al., 2013). Although we did not functionally investigate A $\delta$ -LTMRs fibers here, previous reports using Mibefradil, a nonselective T-type channel blocker, or Cav3.2-KO mice demonstrated that Cav3.2 affects A $\delta$ -LTMR excitability (Wang and Lewin, 2011).

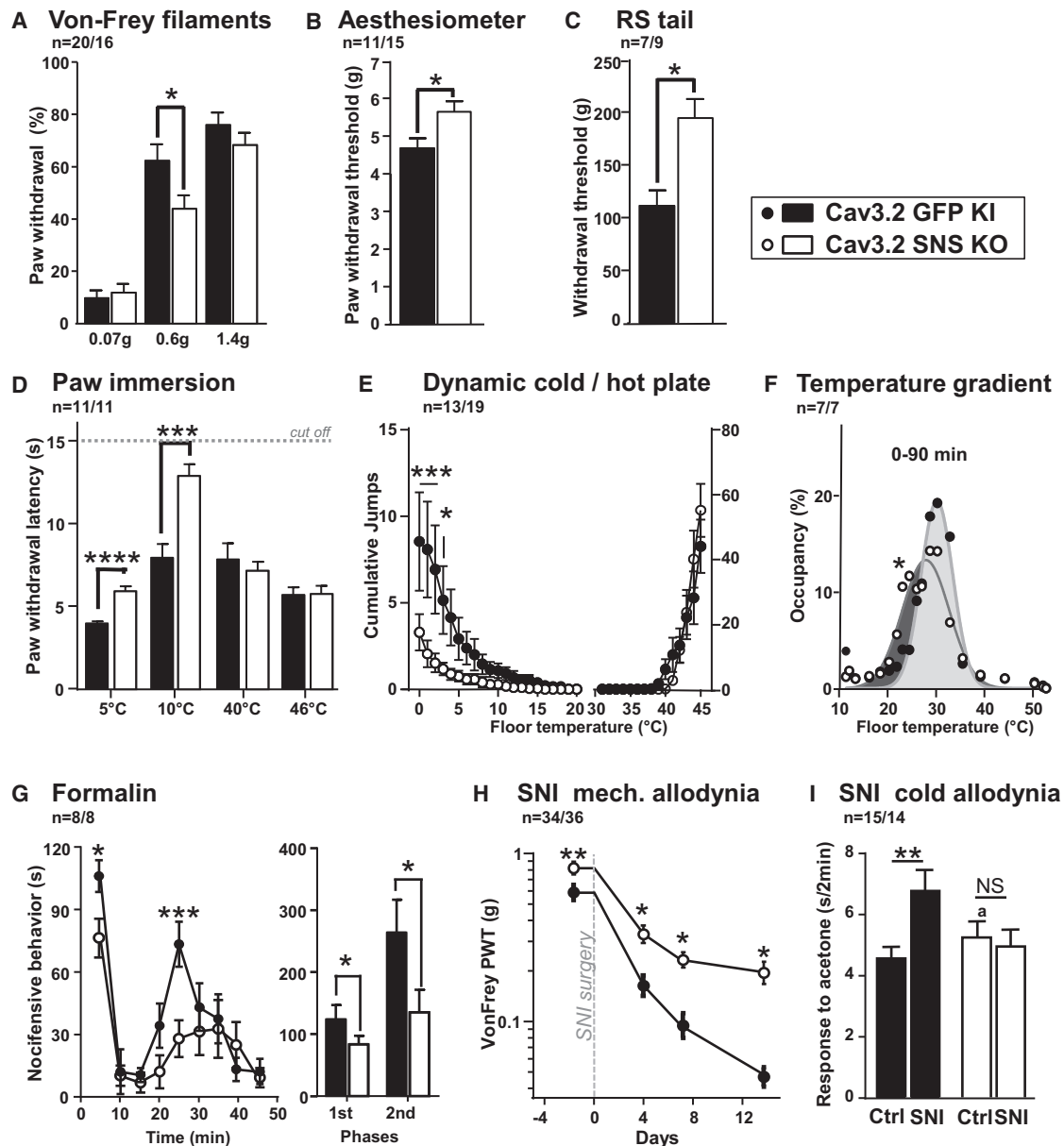


**Figure 7. Acute Light-Touch, Mechanical Cold, and Chemical Pain Deficits and Profound Reduction of Allodynia Produced by Neuropathic Nerve Injury in Cav3.2 SNS KO Mice**

(A–C) Cav3.2-GFP KI and Cav3.2 SNS KO paw withdrawal response to punctate mechanical stimulation of the hindpaw with three distinct von Frey filaments (innocuous 0.07 g, intermediate 0.6 g, and noxious 1.4 g) (A) or with the electronic von Frey apparatus (B) and tail withdrawal to noxious compression with the Randall-Selitto (RS) test (C).

(D) Withdrawal latency to paw immersion in noxious cold (5°C, 10°C) and hot (40°C, 46°C) water.

(E) Responses to dynamic cold and hotplate tests are shown as the cumulative number of jumps for Cav3.2-SNS KO and KI mice according to plate temperature.

(F) Thermotaxis with the temperature gradient test is shown as the time spent by mice on each of these zones for the 90 min duration of the experiment.

(G) Presence of nocifensive behavior (in s) following injection of 2% formalin (10  $\mu$ l) into the hindpaw is recorded in both characteristic phases of this test (first phase from 0 to 10 min, and second phase from 10 to 50 min). Kinetics of the experiment by 5 min intervals (left) and cumulative behavior for both phases (right). (H and I) In the spared nerve injury neuropathic pain model (SNI), mice were tested before (day 2) and after (days 4–14) the surgery for their paw withdrawal response to von Frey filaments (up-and-down method, H) or for their sensitivity to cool stimulation with acetone ejected on the plantar face of hindpaws (cumulative time spent to flick or lick the paw in s [I]).

All data presented are mean  $\pm$  SEM. \* $p < 0.05$  \*\* $p < 0.01$  \*\*\* $p < 0.001$  \*\*\*\* $p < 0.0001$ . “a” indicates nonsignificant (day 2 SNS KO versus GFP KI), Mann-Whitney U test or two-way ANOVA with Bonferroni post hoc test.

DRG neurons are extremely compartmentalized with a very long axonal element representing more than 99% of membrane surface (Devor, 1999). Exploration of Cav3.2-GFP axonal localization revealed two patterns: one confined in the node of Ranvier of A $\delta$ -LTMRs, the other with a diffuse distribution along some thin unmyelinated C-fibers, corresponding presumably to C-LTMRs neurons. In both cases, Cav3.2 is expected to regulate AP conduction parameters. A restricted nodal localization of ion channels is finely controlled by intracellular scaffolds, and the same is also true for the axon initial segment (AIS) in the CNS. Interestingly, T-type channels have been functionally identified in the AIS, thereby tuning neuronal intrinsic plasticity (Bender et al., 2010; Grubb and Burrone, 2010). The function of AIS located T-type channels in the control of neuronal output is certainly conserved for axonal Cav3.2 within unmyelinated regions of DRGs, namely in the nodes of Ranvier for A $\delta$ -LTMRs and along the fibers for C-LTMRs, where they could boost the sodium spike conduction. Investigating the impact of T-type channel blockade on C-LTMRs axonal conduction velocity, we showed that Cav3.2 activity contributes to a faithful conduction of AP. In vivo studies using microneurography showed that C-LTMRs diverge from other C-fibers, with a stable CV upon increased stimulation frequency and some degree of spontaneous activity that leads to efficient sensory information signaling (George et al., 2007). These features might result from the tuning of their excitability by Cav3.2 directly or indirectly via intracellular calcium regulation of other membrane conductances. Elucidating these mechanisms would be particularly interesting in pathological conditions that commonly alter axonal excitability. As a follow up, a dynamic view of Cav3.2 localization will be informative using the properties of the ecliptic-GFP designed to explore such phenomenon.

To complete the picture of Cav3.2 subcellular expression, exploration of central terminals within the dorsal horn corroborated the robustness of the model. Indeed, C-LTMRs and A $\delta$ -LTMRs connect to the ventral lamina Iii and laminae Iii/III, respectively (Li et al., 2011), where Cav3.2-GFP is detected overlapping with the PKC- $\gamma$  labeled layer known to receive LTMR inputs. Moreover, Cav3.2-GFP is also robustly expressed in spinal cord neurons in these regions. Electron microscope analysis within the lamina II confirms the presence of Cav3.2 at both pre- and postsynapses in glomeruli structures. The presynaptic presence substantiates the emerging role of low-voltage-gated calcium influx in neurotransmitters release, including in dorsal horn afferent inputs (García-Caballero et al., 2014; Jacus et al., 2012). Understanding the postsynaptic contribution will need further exploration. Since spinal neuron wiring and function are still largely unknown, visualization of Cav3.2-GFP will be a powerful tool to address such questions.

Finally, the Cav3.2 SNS KO provides insights into its functional significance in C-fibers. First, removing Cav3.2 from C-fibers is dispensable for their development and for their peripheral and central innervations. Furthermore, it does not affect Cav3.2 expression in A $\delta$ -LTMRs or the CNS. We show here that the sensitivity to perceive innocuous and noxious mechanical stimuli is dampened in the SNS KO mice. This phenotype is combined with an altered perception of cold in line with C-LTMR characteristics (Li et al., 2011). Moreover, the early and the late phases of

chemical pain induced by formalin is reduced. This biphasic response is believed to reflect an acute pain in the periphery and then a central sensitization. Yet, recent reevaluation of this scheme emphasized on a peripheral substrate of all the underlying mechanisms (Fischer et al., 2014). This further supports that Cav3.2-expressing peripheral C-LTMRs are important for this behavior, in contrast to many other C-fibers (Shields et al., 2010).

In a pathological context, LTMRs afferents are the prime candidates to support injury-mediated allodynia due to their high cutaneous sensitivity. The weight of clinical data emphasizes the implication of myelinated A- $\beta$  LTMR afferents as the major cellular substrate of allodynia (Campbell et al., 1988). Preclinical findings corroborate this view with cellular and molecular evidences, such as recent data using GFP-delta-opioid-receptor KI mouse (Bardoni et al., 2014). Nevertheless, we show that Cav3.2 channels are not expressed in A $\beta$ -fibers. Additionally, A $\delta$ -LTMRs could also be good candidates. However, these fibers do not seem to be conserved between rodents and humans (Lechner and Lewin, 2013), which also limits somewhat the translational value of murine A $\delta$ -LTMR data. Moreover, in A $\delta$ -fibers, Cav3.2 expression is not reduced in the SNS KO. Finally, the contribution of C-LTMRs to allodynia has emerged from recent studies on C-tactile-fibers both in human patients and in animal models (McGlone et al., 2014; Nagi et al., 2011). Furthermore, unlike A $\beta$ -fibers, C-LTMRs respond to both touch and cooling, consistent with an allodynic phenomenon associated with these two stimuli. Therefore, our data not only demonstrate the contribution of C-tactile-fibers to the pathophysiology of neuropathic pain but also reinforce the status of peripherally expressed Cav3.2 channels as a target of choice for future treatments of mechanical and cold allodynia. These symptoms are commonly associated with multiple neuropathies. Assessing the impact of C-LTMR-expressed Cav3.2 in relevant preclinical models is therefore an important perspective. It is noteworthy that cold allodynia is abolished by intrathecal Cav3.2 antisense treatment in a rat model of diabetic neuropathy (Obradovic et al., 2014). Other compelling data that reinforce our research come from the clinical traits of autism combining impaired social interactions with hypo- or hypertouch and/or cold perception that possibly implicate altered affective function of C-tactile-fibers (Cascio et al., 2008; McGlone et al., 2014). Strikingly, Cav3.2 reduction and gain of function are linked to a range of autism spectrum disorder mutations of the *CACNA1H* gene (Splawski et al., 2006). Whether these mutations affect patients' C-LTMR functions is yet to be elucidated. Thus, allodynia is certainly more complex than involving solely A $\beta$ -fibers, with a likely scenario where other afferents, such as Cav3.2-expressing C-LTMRs, are synergistically orchestrating this maladaptive phenomenon.

Consistent with our study, the VGLUT3 KO that reduces glutamate release from C-LTMRs shows impaired injury-induced mechanical hypersensitivity (Seal et al., 2009), although the phenotype may result from CNS-expressed transporters (Lou et al., 2013). Conversely, in the same fibers, when the release of the analgesic TFAFA4 protein is abolished, pain is exacerbated (Delfini et al., 2013). An attractive hypothesis would be that Cav3.2-mediated calcium influx is important for the release of the pronociceptive glutamate but dispensable for TFAFA4 secretion. Moreover, the proexcitatory effect of Cav3.2 contributes to

the efficient firing of C-LTMRs and the subsequent release of glutamate, further amplified presynaptically by low-voltage-gated calcium entry. In a neuropathic states, a change in the analgesic/painful balance of C-LTMR signaling could largely support allodynia, with a potential reduction of TFAA4 secretion resulting in central disinhibition, combined with an increased Cav3.2 membrane expression exacerbating pain signaling from the periphery. However, the conditional Runx1 KO driven by the VGLUT3-Cre shows that the altered distal skin innervation and mechanosensitivity of VGLUT3-positive C-LTMRs does not affect acute and pathological pain (even though cold nociception was not assessed) (Lou et al., 2013). One possible reconciliation with our results is that the Cav3.2-expressing C-LTMR population is broader than the persistent VGLUT3-expressing DRGs and that Cav3.2 removal from VGLUT3-negative C-LTMRs contributes to the phenotype described here. The use of a more cell-specific Cav3.2 ablation would be necessary to resolve this issue.

The Cav3.2 SNS KO phenotype agrees with what is expected from the channel loss in C-LTMR fibers. However, it is distinct from the pain phenotype of the complete channel deletion in the null mice (Choi et al., 2007) or in all DRG and some spinal neurons in rats with intrathecal antisense-mediated Cav3.2 knock-down (Bourinet et al., 2005; Messinger et al., 2009) regarding noxious heat perception. Interestingly, we demonstrate that heat-evoked pain is retained when Cav3.2 is deleted only in Nav1.8-positive DRGs, a phenotype reminiscent of conditional ablation of different genes in the same neuronal population. Thus, additional roles of Cav3.2 may be mediated through neurons that do not express Nav1.8 (in A $\delta$ -LTMRs in a few Nav1.8-negative C-fibers, or likely within spinal and supraspinal pain pathways). Deciphering all the sensory modalities associated with different sets of Cav3.2-expressing cells will require additional specific conditional ablations.

In conclusion, we provide evidence that LTMR subtypes innervating the majority of hair subtypes in the skin rely on Cav3.2 channel functioning for their high sensitivity to detect, faithfully conduct, and transfer tactile/pain information. This peculiarity may result from a common global specification program of A $\delta$ - and C-LTMRs, ranging from the expression of specific molecular markers, including Cav3.2 in their portfolio of ion channels, to their anatomy and functional organization (Li et al., 2011; Lou et al., 2013). Since LTMRs neurons play a crucial role in the pathophysiology of multiple chronic pain syndromes linked to allodynia, hypersensitivity, and spontaneous pain that are largely resistant to present therapies, these data further validate the utility of pharmacologically inhibiting Cav3.2 to improve quality of life.

## EXPERIMENTAL PROCEDURES

### Mice Lines

To generate Cav3.2-GFP KI mice, we used the bacterial artificial chromosome-based homologous recombination in embryonic stem cells. The Nav1.8-Cre and the Venus-TFAA4 mice lines had been described previously (see the Supplemental Experimental Procedures for details).

### Immunohistochemistry

Immunohistochemistry on tissue sections, in situ hybridization, hairy skin whole-mount immunohistochemistry, and teased fiber labeling were per-

formed using standard methods (see the Supplemental Experimental Procedures for details).

### Electrophysiology

Mouse DRGs were prepared as described previously. Cav3.2 GFP+ positive neurons were identified from their extracellular GFP with live staining using mouse anti-GFP immunoglobulin G (IgG) (1/100, 5 min, Roche) and Alexa 488-coupled anti-mouse IgG (1/300, 5 min, Invitrogen). Voltage-gated calcium currents, MA currents, or membrane potentials were recorded as in Delfini et al. (2013) and Francois et al. (2013). The isolated paw hairy skin-saphenous nerve preparation and single-fiber recording were used as previously described (see the Supplemental Experimental Procedures for details).

### Behavioral Assays

Experiments were conducted at room temperature with 8- to 12-week-old littermate males and with both genders for neuropathic pain. Animals were acclimated to their testing environment prior to all experiments. Experimenters were blind to the genotype during testing. Pain scores were determined with strict adherence to ethical guidelines (Zimmermann, 1983) and in respect to local ethical committee (see the Supplemental Experimental Procedures for details).

## SUPPLEMENTAL INFORMATION

Supplemental Information includes Supplemental Experimental Procedures and seven figures and can be found with this article online at <http://dx.doi.org/10.1016/j.celrep.2014.12.042>.

## AUTHOR CONTRIBUTIONS

A.F., N.S., S.L., O.P., and E.B. designed the experiments. A.F., N.S., S.L., A.P., J.S., S.D., A.M., J.N., and E.B. performed the experiments. J.W. provided reagents. A.F., N.S., S.L., A.P., S.D., A.D., J.N., O.P., and E.B. analyzed the data. A.F., A.M., O.P., and E.B. wrote the manuscript.

## ACKNOWLEDGMENTS

We are grateful to Montpellier RIO imaging; C. Cazevielle and C. Sanchez for TEM microscopy (CRIC, Montpellier); J. Rothman for ecliptic GFP cDNA; V. Uebele (Merck) for the TTA-A2; R. Seal for VGLUT3-GFP mice DRGs; L. Gouttebroze, J. Devaux, and P. Carroll for antibodies; and C. Barrère, J. Guillemin, C. Jopling, and N. Lamb for assistance. This work was supported by grants from the ANR (ANR-09-MNPS-037, ANR-08-NMPS-025), the AFM (AFM-PainT) to E.B., and by a grant of the Deutsche Forschungsgemeinschaft Po137/42-1 to O.P. and N.S. A.F., S.L., and J.S. are supported by fellowships from the French ministry of research and education, the AFM, the Labex ICST, and the FRM.

Received: October 27, 2014

Revised: November 14, 2014

Accepted: December 18, 2014

Published: January 15, 2015

## REFERENCES

- Abrahamsen, B., Zhao, J., Asante, C.O., Cendan, C.M., Marsh, S., Martinez-Barbera, J.P., Nassar, M.A., Dickenson, A.H., and Wood, J.N. (2008). The cell and molecular basis of mechanical, cold, and inflammatory pain. *Science* 321, 702–705.
- Abraira, V.E., and Ginty, D.D. (2013). The sensory neurons of touch. *Neuron* 79, 618–639.
- Bardoni, R., Tawfik, V.L., Wang, D., François, A., Solorzano, C., Shuster, S.A., Choudhury, P., Betelli, C., Cassidy, C., Smith, K., et al. (2014). Delta opioid receptors presynaptically regulate cutaneous mechanosensory neuron input to the spinal cord dorsal horn. *Neuron* 81, 1312–1327.

- Basbaum, A.I., Bautista, D.M., Scherrer, G., and Julius, D. (2009). Cellular and molecular mechanisms of pain. *Cell* 139, 267–284.
- Bender, K.J., Ford, C.P., and Trussell, L.O. (2010). Dopaminergic modulation of axon initial segment calcium channels regulates action potential initiation. *Neuron* 68, 500–511.
- Bessou, P., Burgess, P.R., Perl, E.R., and Taylor, C.B. (1971). Dynamic properties of mechanoreceptors with unmyelinated (C) fibers. *J. Neurophysiol.* 34, 116–131.
- Bourinet, E., Alloui, A., Monteil, A., Barrère, C., Couette, B., Poirat, O., Pages, A., McRory, J., Snutch, T.P., Eschalièr, A., and Nargeot, J. (2005). Silencing of the Cav3.2 T-type calcium channel gene in sensory neurons demonstrates its major role in nociception. *EMBO J.* 24, 315–324.
- Bourinet, E., Altier, C., Hildebrand, M.E., Trang, T., Salter, M.W., and Zamponi, G.W. (2014). Calcium-permeable ion channels in pain signaling. *Physiol. Rev.* 94, 81–140.
- Brumovsky, P., Villar, M.J., and Hökfelt, T. (2006). Tyrosine hydroxylase is expressed in a subpopulation of small dorsal root ganglion neurons in the adult mouse. *Exp. Neurol.* 200, 153–165.
- Campbell, J.N., Raja, S.N., Meyer, R.A., and Mackinnon, S.E. (1988). Myelinated afferents signal the hyperalgesia associated with nerve injury. *Pain* 32, 89–94.
- Cascio, C., McGlone, F., Folger, S., Tannan, V., Baranek, G., Pelphrey, K.A., and Essick, G. (2008). Tactile perception in adults with autism: a multidimensional psychophysical study. *J. Autism Dev. Disord.* 38, 127–137.
- Choe, W., Messinger, R.B., Leach, E., Eckle, V.S., Obradovic, A., Salajegheh, R., Jevtovic-Todorovic, V., and Todorovic, S.M. (2011). TTA-P2 is a potent and selective blocker of T-type calcium channels in rat sensory neurons and a novel antinociceptive agent. *Mol. Pharmacol.* 80, 900–910.
- Choi, S., Na, H.S., Kim, J., Lee, J., Lee, S., Kim, D., Park, J., Chen, C.C., Campbell, K.P., and Shin, H.S. (2007). Attenuated pain responses in mice lacking Ca(V)3.2 T-type channels. *Genes Brain Behav.* 6, 425–431.
- Coste, B., Crest, M., and Delmas, P. (2007). Pharmacological dissection and distribution of Na<sup>v</sup>/Nav1.9, T-type Ca<sup>2+</sup> currents, and mechanically activated cation currents in different populations of DRG neurons. *J. Gen. Physiol.* 129, 57–77.
- Decosterd, I., and Woolf, C.J. (2000). Spared nerve injury: an animal model of persistent peripheral neuropathic pain. *Pain* 87, 149–158.
- Delfini, M.C., Mantilleri, A., Gaillard, S., Hao, J., Reynders, A., Malapert, P., Alonso, S., François, A., Barrère, C., Seal, R., et al. (2013). TFAFA4, a chemokine-like protein, modulates injury-induced mechanical and chemical pain hypersensitivity in mice. *Cell Rep.* 5, 378–388.
- Delmas, P., Hao, J., and Rodat-Despoix, L. (2011). Molecular mechanisms of mechanotransduction in mammalian sensory neurons. *Nat. Rev. Neurosci.* 12, 139–153.
- Devor, M. (1999). Unexplained peculiarities of the dorsal root ganglion. *Pain* 6 (6), S27–S35.
- Fischer, M., Carli, G., Raboisson, P., and Reeh, P. (2014). The interphase of the formalin test. *Pain* 155, 511–521.
- François, A., Kerckhove, N., Meleine, M., Alloui, A., Barrère, C., Gelot, A., Uebele, V.N., Renger, J.J., Eschalièr, A., Ardid, D., and Bourinet, E. (2013). State-dependent properties of a new T-type calcium channel blocker enhance Ca(V)3.2 selectivity and support analgesic effects. *Pain* 154, 283–293.
- François, A., Laffray, S., Pizzoccaro, A., Eschalièr, A., and Bourinet, E. (2014). T-type calcium channels in chronic pain: mouse models and specific blockers. *Pflugers Arch.* 466, 707–717.
- García-Caballero, A., Gadotti, V.M., Stenkowski, P., Weiss, N., Souza, I.A., Hodgkinson, V., Bladen, C., Chen, L., Hamid, J., Pizzoccaro, A., et al. (2014). The deubiquitinating enzyme USP5 modulates neuropathic and inflammatory pain by enhancing Cav3.2 channel activity. *Neuron* 83, 1144–1158.
- George, A., Serra, J., Navarro, X., and Bostock, H. (2007). Velocity recovery cycles of single C fibres innervating rat skin. *J. Physiol.* 578, 213–232.
- Grubb, M.S., and Burrone, J. (2010). Activity-dependent relocation of the axon initial segment fine-tunes neuronal excitability. *Nature* 465, 1070–1074.
- Hall, D.H., and Treinin, M. (2011). How does morphology relate to function in sensory arbors? *Trends Neurosci.* 34, 443–451.
- Jacus, M.O., Uebele, V.N., Renger, J.J., and Todorovic, S.M. (2012). Presynaptic Cav3.2 channels regulate excitatory neurotransmission in nociceptive dorsal horn neurons. *J. Neurosci.* 32, 9374–9382.
- Jagodic, M.M., Pathirathna, S., Joksovic, P.M., Lee, W., Nelson, M.T., Naik, A.K., Su, P., Jevtovic-Todorovic, V., and Todorovic, S.M. (2008). Upregulation of the T-type calcium current in small rat sensory neurons after chronic constrictive injury of the sciatic nerve. *J. Neurophysiol.* 99, 3151–3156.
- Lallemend, F., and Ernfor, P. (2012). Molecular interactions underlying the specification of sensory neurons. *Trends Neurosci.* 35, 373–381.
- Lechner, S.G., and Lewin, G.R. (2013). Hairy sensation. *Physiology (Bethesda)* 28, 142–150.
- Li, L., Rutlin, M., Abraira, V.E., Cassidy, C., Kus, L., Gong, S., Jankowski, M.P., Luo, W., Heintz, N., Koerber, H.R., et al. (2011). The functional organization of cutaneous low-threshold mechanosensory neurons. *Cell* 147, 1615–1627.
- Liu, Y., and Ma, Q. (2011). Generation of somatic sensory neuron diversity and implications on sensory coding. *Curr. Opin. Neurobiol.* 21, 52–60.
- Lou, S., Duan, B., Vong, L., Lowell, B.B., and Ma, Q. (2013). Runx1 controls terminal morphology and mechanosensitivity of VGLUT3-expressing C-mechanoreceptors. *J. Neurosci.* 33, 870–882.
- Marger, F., Gelot, A., Alloui, A., Matricon, J., Ferrer, J.F., Barrère, C., Pizzoccaro, A., Muller, E., Nargeot, J., Snutch, T.P., et al. (2011). T-type calcium channels contribute to colonic hypersensitivity in a rat model of irritable bowel syndrome. *Proc. Natl. Acad. Sci. USA* 108, 11268–11273.
- McGlone, F., Wessberg, J., and Olsson, H. (2014). Discriminative and affective touch: sensing and feeling. *Neuron* 82, 737–755.
- Messinger, R.B., Naik, A.K., Jagodic, M.M., Nelson, M.T., Lee, W.Y., Choe, W.J., Orestes, P., Latham, J.R., Todorovic, S.M., and Jevtovic-Todorovic, V. (2009). In vivo silencing of the Ca(V)3.2 T-type calcium channels in sensory neurons alleviates hyperalgesia in rats with streptozocin-induced diabetic neuropathy. *Pain* 145, 184–195.
- Miesenböck, G., De Angelis, D.A., and Rothman, J.E. (1998). Visualizing secretion and synaptic transmission with pH-sensitive green fluorescent proteins. *Nature* 394, 192–195.
- Mills, C., Leblond, D., Joshi, S., Zhu, C., Hsieh, G., Jacobson, P., Meyer, M., and Decker, M. (2012). Estimating efficacy and drug ED50's using von Frey thresholds: impact of weber's law and log transformation. *J. Pain* 13, 519–523.
- Nagi, S.S., Rubin, T.K., Chelvanayagam, D.K., Macefield, V.G., and Mahns, D.A. (2011). Allodynia mediated by C-tactile afferents in human hairy skin. *J. Physiol.* 589, 4065–4075.
- Obradovic, A.L., Hwang, S.M., Scarpa, J., Hong, S.J., Todorovic, S.M., and Jevtovic-Todorovic, V. (2014). CaV3.2 T-type calcium channels in peripheral sensory neurons are important for mibefradil-induced reversal of hyperalgesia and allodynia in rats with painful diabetic neuropathy. *PLoS ONE* 9, e91467.
- Peng, Y.B., Ringkamp, M., Campbell, J.N., and Meyer, R.A. (1999). Electrophysiological assessment of the cutaneous arborization of Adelta-fiber nociceptors. *J. Neurophysiol.* 82, 1164–1177.
- Perez-Reyes, E. (2003). Molecular physiology of low-voltage-activated t-type calcium channels. *Physiol. Rev.* 83, 117–161.
- Rose, K.E., Lunardi, N., Boscolo, A., Dong, X., Erisir, A., Jevtovic-Todorovic, V., and Todorovic, S.M. (2013). Immunohistological demonstration of CaV3.2 T-type voltage-gated calcium channel expression in soma of dorsal root ganglion neurons and peripheral axons of rat and mouse. *Neuroscience* 250, 263–274.
- Seal, R.P., Wang, X., Guan, Y., Raja, S.N., Woodbury, C.J., Basbaum, A.I., and Edwards, R.H. (2009). Injury-induced mechanical hypersensitivity requires C-low threshold mechanoreceptors. *Nature* 462, 651–655.

- Shields, S.D., Cavanaugh, D.J., Lee, H., Anderson, D.J., and Basbaum, A.I. (2010). Pain behavior in the formalin test persists after ablation of the great majority of C-fiber nociceptors. *Pain* 151, 422–429.
- Shin, J.B., Martinez-Salgado, C., Heppenstall, P.A., and Lewin, G.R. (2003). A T-type calcium channel required for normal function of a mammalian mechanoreceptor. *Nat. Neurosci.* 6, 724–730.
- Splawski, I., Yoo, D.S., Stotz, S.C., Cherry, A., Clapham, D.E., and Keating, M.T. (2006). CACNA1H mutations in autism spectrum disorders. *J. Biol. Chem.* 281, 22085–22091.
- Stirling, L.C., Forlani, G., Baker, M.D., Wood, J.N., Matthews, E.A., Dickenson, A.H., and Nassar, M.A. (2005). Nociceptor-specific gene deletion using heterozygous Nav1.8-Cre recombinase mice. *Pain* 113, 27–36.
- Takahashi, K., Sato, J., and Mizumura, K. (2003). Responses of C-fiber low threshold mechanoreceptors and nociceptors to cold were facilitated in rats persistently inflamed and hypersensitive to cold. *Neurosci. Res.* 47, 409–419.
- Takahashi, T., Aoki, Y., Okubo, K., Maeda, Y., Sekiguchi, F., Mitani, K., Nishikawa, H., and Kawabata, A. (2010). Upregulation of Ca(v)3.2 T-type calcium channels targeted by endogenous hydrogen sulfide contributes to maintenance of neuropathic pain. *Pain* 150, 183–191.
- Talley, E.M., Cribbs, L.L., Lee, J.H., Daud, A., Perez-Reyes, E., and Bayliss, D.A. (1999). Differential distribution of three members of a gene family encoding low voltage-activated (T-type) calcium channels. *J. Neurosci.* 19, 1895–1911.
- Vallbo, A.B., Olausson, H., and Wessberg, J. (1999). Unmyelinated afferents constitute a second system coding tactile stimuli of the human hairy skin. *J. Neurophysiol.* 81, 2753–2763.
- Vrontou, S., Wong, A.M., Rau, K.K., Koerber, H.R., and Anderson, D.J. (2013). Genetic identification of C fibres that detect massage-like stroking of hairy skin in vivo. *Nature* 493, 669–673.
- Wang, R., and Lewin, G.R. (2011). The Cav3.2 T-type calcium channel regulates temporal coding in mouse mechanoreceptors. *J. Physiol.* 589, 2229–2243.
- Woodbury, C.J., Ritter, A.M., and Koerber, H.R. (2001). Central anatomy of individual rapidly adapting low-threshold mechanoreceptors innervating the “hairy” skin of newborn mice: early maturation of hair follicle afferents. *J. Comp. Neurol.* 436, 304–323.
- Wu, H., Williams, J., and Nathans, J. (2012). Morphologic diversity of cutaneous sensory afferents revealed by genetically directed sparse labeling. *eLife* 1, e00181.
- Zimmermann, M. (1983). Ethical guidelines for investigations of experimental pain in conscious animals. *Pain* 16, 109–110.
- Zimmermann, K., Leffler, A., Babes, A., Cendan, C.M., Carr, R.W., Kobayashi, J., Nau, C., Wood, J.N., and Reeh, P.W. (2007). Sensory neuron sodium channel Nav1.8 is essential for pain at low temperatures. *Nature* 447, 855–858.